



The Technique of Analyzing a Non-Homogeneous Partial Differential Equation by Splitting The Problem into The Inverse and Direct Problems

Shnyar Ali Rashid^{1*}, Shilan O. Hussein²

1,2 Department of mathematics, College of science, University of Sulaymaniyah, Sulaymaniyah, Iraq

shnyar.rashid@univsul.edu.iq^{1*}; shilan.husen@univsul.edu.iq²

Corresponding author email: shnyar.rashid@univsul.edu.iq^{1}; mobile: 07731228787

تقنية تحليل المعادلة التفاضلية الجزئية غير المتجانسة بتقسيم المسألة إلى

مسألة عكسية ومسألة مباشرة

شنيار علي رشيد^{1*}, شيلان عثمان حسين²

¹ - ² قسم الرياضيات، كلية العلوم، جامعة السليمانية، السليمانية، العراق

Accepted:

24/12/2025

Published:

31/12/2025

ABSTRACT:

Background: In this study, we decompose a non-homogeneous second-order partial differential equation into a homogeneous part and a non-homogeneous part. Previous research on the existence and uniqueness of solutions for both sections provide a clear mathematical foundation. The main goal of this research is to divide the partial differential equation into two separate parts: one homogeneous and one non-homogeneous. These parts are then addressed using initial conditions along with various boundary and overdetermination conditions.

Materials and Methods: We use the finite difference method to numerically solve both the homogeneous and non-homogeneous components. Various boundary conditions are considered, including Dirichlet, Neumann, and mixed conditions, each requiring specific supplementary information. To assess the stability of the numerical solutions, we introduce different noise levels and apply Tikhonov regularization to stabilize the results.

Results: Several numerical examples are presented to evaluate the effectiveness of the proposed approach. The findings indicate that the finite difference method yields accurate solutions under a range of boundary conditions, and that Tikhonov regularization effectively enhances stability in noisy environments.

Conclusion: The numerical results validate the robustness and reliability of the proposed method. By combining Tikhonov regularization with finite difference discretization, this study establishes an efficient framework for solving non-homogeneous second-order partial differential equations under various boundary conditions. The research results indicate that, under various boundary, extra, and initial conditions, we can solve the problem and find convergent solutions for both parts.

Keywords: Inverse and direct problem; Finite difference method; Regularization; Second-order partial differential equation.

1. INTRODUCTION

Partial Differential Equations (PDEs) are fundamental mathematical models describing a wide range of physical, biological, and engineering phenomena involving functions of several independent variables and their partial derivatives. They naturally arise in processes where quantities vary continuously in both space and time, such as heat conduction, wave propagation, fluid dynamics, quantum mechanics, and elasticity theory. Mathematically, a PDE involves an unknown function and its partial derivatives with respect to spatial and temporal variables. PDEs are typically classified by order, linearity, and type: elliptic PDEs (e.g., Laplace's equation) describe steady-state phenomena such as electrostatics and incompressible fluid flow; parabolic PDEs (e.g., the heat equation) model diffusive processes with gradual temporal changes; and hyperbolic PDEs (e.g., the wave equation) represent dynamic systems with finite propagation speeds, such as vibrations, acoustic waves, and seismic activity. This study addresses an inverse force problem for the one-dimensional non-homogeneous second-order hyperbolic PDE, aiming to reconstruct a spatially dependent force function from observed data. To ensure uniqueness, the forcing function is assumed to depend only on the spatial variable. Theoretical guarantees for uniqueness and continuous dependence on data were established in [1], which also introduced optimization-based techniques such as linear programming and least squares. The Boundary Element Method (BEM) and the Finite Element Method (FEM) are numerical techniques used to solve partial differential equations and have been widely studied in the literature. For example, BEM has been employed to address partial differential equations (wave equation) with a constant wave speed by using the fundamental solution [2],[15], especially when the force term is free. However, these methods become less suitable when dealing with variable wave speeds or non-free force terms. Therefore, in order to extend this range of applicability, in this paper the numerical method for discretizing the partial differential equations (wave equation) is the finite difference method (FDM). Previous works have explored related problems using a various of methods. For instance, [2] employed the Boundary Element Method (BEM) with Dirichlet boundary conditions, while [3],[4],[5],[6] applied a hybrid BEM and Finite Difference Method (FDM) approach. Some studies [1],[3],[7] used separation of variables to discretize the wave equation under the assumption of constant wave speed. In contrast, this work applies the Finite Difference Method exclusively for both the direct and inverse problems. The choice of FDM is motivated by its simplicity, ease of implementation, and effectiveness for time-dependent PDEs. The problem is decomposed via the principle of superposition into two parts: Part one: A direct problem with a zero forcing term. Second part: An inverse problem with homogeneous boundary and initial conditions, which, reduces to a linear least-squares system. A problem "part one" is considered well-posed, according to literature, if it satisfies three criteria: the solution exists for all given data, it is unique, and it depends continuously on the data (stability), meaning that small errors in the input result in only small errors in the output. The problem "second part" is called ill-posed if any of these criteria are not met, meaning it may have no solution, multiple solutions, or unstable solutions—where even minor errors in the input can cause extremely large errors in the output. Most difficulties in solving these problems arise from this fundamental instability [17]-[19].

Because inverse problems are inherently ill-posed, this system is ill-conditioned because small boundary data errors can cause significant force errors. Tikhonov regularization improves stability, with the regularization parameter chosen based on the norm error. Numerical results show the method provides stable, reliable outcomes. Moreover, we employ zeroth-order Tikhonov regularization [8],



with the regularization parameter chosen via the norm error criterion [2]. Several boundary condition types, Dirichlet, Neumann, and mixed, are investigated. In mixed cases, one well-known boundary condition is prescribed while the displacement at the opposite boundary is treated as additional input data.

To evaluate stability, controlled noise is added to the synthetic data. The impact of noise and the effectiveness of the regularization strategy are analyzed numerically [9] and [10]. This work extends previous studies by introducing alternative supplementary data and boundary conditions, allowing assessment of their effect on reconstruction accuracy, an aspect not addressed in [2],[3],[4],[6],[7]. The proposed method demonstrates high accuracy and consistency, with results remain stable under various conditions, confirming the reliability of the approach.

The remainder of the paper is organized as follows: Section 2 presents the mathematical formulation of the problem, Section 3 discusses numerical results and analysis, and Section 4 concludes the study.

2. MATHEMATICAL FORMULATION:

The mathematical model describing the vibration of a bounded structure subjected to an external force is governed by the classical non-homogeneous partial equation, as presented in [2],[3],[5],[11],[16]:

$$u_{tt} = c^2 u_{xx} + f(x), \quad x \in (0, L) \times (0, T), \quad T > 0 \quad (1)$$

$$u(x, 0) = u_0(x), \quad u_t(x, 0) = v_0(x), \quad x \in [0, L], \quad (2)$$

equation (2) gives the initial condition, and this study has looked at six different cases for the boundary conditions, with an extra condition as follows:

- Boundary condition I (BCI):

$$u(0, t) = p_0(t), \quad u(L, t) = p_L(t), \quad t \in [0, T] \quad (3)$$

$$u_x(L, t) = q_L(t), \quad t \in [0, T] \quad (4)$$

- Boundary condition II (BCII):

$$u(0, t) = p_0(t), \quad u_x(L, t) = q_L(t), \quad t \in [0, T] \quad (5)$$

$$u(L, t) = p_L(t), \quad t \in [0, T] \quad (6)$$

- Boundary condition III (BCIII): Using the same boundary condition (3) from BCI, plus an extra condition:

$$u_x(0, t) = q_0(t), \quad t \in [0, T] \quad (7)$$

- Boundary condition IV (BCIV):

$$u_x(0, t) = q_0(t), \quad u(L, t) = p_L(t), \quad t \in [0, T] \quad (8)$$

$$u(0, t) = p_0(t), \quad t \in [0, T] \quad (9)$$

- Boundary condition V (BCV): we are using the same boundary condition (8) from BCIV, along with an extra condition that is specific to this problem:

$$u(x, T) = u_T(x), \quad x \in [0, L], \quad T > 0 \quad (10)$$



- Boundary condition VI (BCIV): both the additional criterion (10) and the boundary condition (5) from the BCII have been implemented here.

Where $\{x, t, u, u_0, v_0\}$ variables denote {space, time, displacement, starting displacement, velocity}, respectively. Equation (3) represents Dirichlet boundary conditions; equations (5) and (8) correspond to mixed boundary conditions; while equations (4), (6), (7), (9), and (10) provide additional data conditions. Table 1 outlines all six problems, clearly stating the boundary conditions and the additional conditions applied in this study.

Table 1. Non-homogeneous partial equation with six different boundary conditions and additional conditions.

Main Problem	$u_{tt} = c^2 u_{xx} + f(x)$					
ICs	$u(x, 0) = u_0(x), \quad u_t(x, 0) = v_0(x)$					
BCI	BCII	BCIII	BCIV	BCV	BCVI	
$u(0, t) = p_0(t)$	$u(0, t) = p_0(t)$	$u(0, t) = p_0(t)$	$u_x(0, t) = q_0(x)$	$u_x(0, t) = q_0(x)$	$u(0, t) = p_0(t)$	
$u(L, t) = p_L(t)$	$u_x(L, t) = q_L(t)$	$u(L, t) = p_L(t)$	$u(L, t) = p_L(t)$	$u(L, t) = p_L(t)$	$u_x(L, t) = q_L(t)$	
Extra Condition						
$u_x(L, t) = q_L(t)$	$u(L, t) = p_L(t)$	$u_x(0, t) = q_0(t)$	$u(0, t) = p_0(t)$	$u(x, T) = u_T(x)$	$u(x, T) = u_T(x)$	

This study examines a non-homogeneous PDE (u, f) as both a direct and an inverse problem. When f is known, it forms the direct **problems (1)** and **(2)**, such that: **Problems 1** and **3** uses (3), **Problems 2** and **6** use (5), and **Problems 4** and **5** use (8) as a boundary condition. And if f is unknown, additional conditions are needed to figure out (u, f): **Problem 1** uses equation (4), **Problem 2** uses equation (6), **Problem 3** uses equation (7), **Problem 4** uses equation (9), and **Problems 5** and **6** use equation (10).

For existence and uniqueness, this research relies on the theorems and requirements outlined in [2]-[5],[7],[10],[11]. We assume that all conditions are as functions of time over the interval $T > 0$, except for the last condition, which is enforced in terms of x . The goal of the inverse problem is to find the pair $(u(x, t), f(x))$ that satisfies equations (1)-(10). Note that $f(x)$ must depend only on x ; if $f(x)$ also depends on t , then $u(x, t)$ can be modified by adding a term of the form $(t^2 x^2 (x - L)^2 U(x, t))$, where $U \in C^{2,1}[0, L] \times [0, \infty]$, resulting in a different solution. Although equation (10) includes x , the other measurements (4), (6), (7), and (9) depend on time, while the unknown force $f(x)$ in this context is a function of space. Cannon and Dunninger (1970) [1] also showed that problems (1)-(10) have at most one solution, ensuring uniqueness, and provided additional supporting theorems in [12],[13] as follows:

Theorem 1 [12]. Assume that $\Omega \subset R^n$ is boundary star-shaper domain with a sufficiently smooth boundary such that $T > \text{diam}(\Omega)$, such that $u_{tt}(x, t) = \nabla^2 u(x, t) + f(x)h(x, t)$, $(x, t) \in \Omega \times (0, T)$). Then the inverse problem (2)-(10) has at most one solution $(u(x, t), f(x))$, where $h = 1$ and

1) $h \in H^2(0, T; L^\infty(\Omega))$ be such that $h(., 0) \in L^\infty(\Omega)$, $h_t(., 0) \in L^\infty(\Omega)$ and



$H := \frac{\|h_{tt}\|_{L^2(0,T;L^\infty(\Omega))}}{\inf_{x \in \Omega} |h(x,0)|}$ is sufficiently small.

- 2) $u \in L^2(0, T; H^1(\Omega))$, $u_t \in L^2(0, T; L^2(\Omega))$, $u_{tt} \in L^2(0, T; H^1(\Omega)'), f \in L^2(\Omega)$, where $\Gamma = \partial\Omega$
- 3) The Neumann observation $(\partial_x(x, t) = q(x, t), (x, t) \in \Gamma \times \partial\Omega(0, T))$ must be applied throughout the entire boundary $\Gamma = \partial\Omega$ in order for the previously mentioned uniqueness Theorem (1) to hold.

Theorem 2 [13]. Assume that $\Omega \subset \mathbb{R}^n$ is a bounded star-shaped domain with smooth boundary such that $T > \text{diam}$. Let $h \in C^1[0, T]$ be independent of x such that equation

$(u_{tt}(x, t) = \nabla^2 u(x, t) + f(x)h(x, t), (x, t) \in \Omega \times (0, T))$ becomes:

$$u_{tt}(x, t) = \nabla^2 u(x, t) + f(x)h(x), \quad (x, t) \in \Omega \times (0, T)$$

and assume further that $h(0) \neq 0$. Then the inverse problem

$$\begin{aligned} u(x, 0) &= \varphi(x), \quad x \in \Omega & u_t(x, 0) &= \psi(x), \quad x \in \Omega \\ u(x, t) &= p(x, t), \quad (x, t) \in \partial\Omega \times (0, T), & \frac{\partial u}{\partial \nu}(x, t) &= q(x, t), \quad (x, t) \in \Gamma \times (0, T) \end{aligned}$$

And equation (24) has at most one solution in the class of functions

$$u \in C^1([0, T]; H^1(\Omega)) \cap C^2([0, T]; L^2(\Omega)), \quad f \in L^2(\Omega),$$

in above equation $C^m([0, T]; X)$, where $m \in \{1, 2\}$ and $X \in \{H^1(\Omega), L^2(\Omega)\}$, denotes the space of m -times continuously differentiable functions defined on $[0, T]$ with values in X .

To approach **Problems (1)** and **(2)**, is split u into $v + w$ [1]-[4]: (i) the direct problem $v(x, t)$ satisfies the homogeneous partial differential equation $v_{tt} = v_{xx}$, subject to the same initial and boundary conditions as in the preceding above problems. (ii) the inverse problem $w_{tt} = w_{xx} + f(x)$, with the zero initial condition and the boundary conditions, and include an extra condition for each problem as follows, where $t \in [0, T]$ and $x \in [0, L]$:

- **Problem 1:** $w_x(L, t) = q_L(t) - v_x(L, t)$,
- **Problem 2:** $w(L, t) = p_L(t) - v(L, t)$,
- **Problem 3:** $w_x(0, t) = q_0(t) - v_x(0, t)$,
- **Problem 4:** $w(0, t) = p_0(t) - v(0, t)$,
- **Problems 5 and 6:** $w(x, T) = u_T(x) - v(x, T)$.

Furthermore, Table 2 illustrates how the partial differential equations are divided into direct and inverse problems, including the six boundary and additional conditions relevant to each.



Table 2. Splitting the non-homogeneous partial equation into direct and inverse problems with initial and six boundary and extreme conditions

$u = v + w$					
$v(x, t)$ satisfies the direct problem $v_{tt} = v_{xx}$			w satisfies the inverse problem $w_{tt} = w_{xx} + f(x)$		
subject to the same initial and boundary conditions as in Table 1			with the zero initial condition and the boundary conditions		
Extra condition					
Problem 1	Problem 2	Problem 3	Problem 4	Problem 5	Problem 6
$w_x(L, t) = q_L(t) - v_x(L, t)$	$w(L, t) = p_L(t) - v(L, t)$	$w_x(0, t) = q_0(t) - v_x(0, t)$	$w(0, t) = p_0(t) - v(0, t)$	$w(x, T) = u_T(x) - v(x, T)$	$w(x, T) = u_T(x) - v(x, T)$

Algorithm for Solving Equation (1)

- **Step 1:** Solve the homogeneous equation $v_{tt} = v_{xx}$ (direct problem) using the same initial and boundary conditions as Equation (1) to determine v and any additional conditions needed.
- **Step 2:** Using the extra conditions from Step 1, solve the nonhomogeneous equation $w_{tt} = w_{xx} + f(x)$ (inverse problem) with zero initial and boundary conditions. After discretization, a linear system is created and simplified (due to linearity) to find the source term $f(x)$. Once $f(x)$ is determined, w is computed.
- **Step 3:** Use $u = v + w$ to find the solution to the original problem (1).
- **Step 4:** Because the inverse problem is ill-posed, noise is added to the additional condition to evaluate stability. Tikhonov regularization is employed to stabilize the solution.

The following section and numerical examples provide an explanation of how this algorithm and its steps work in detail.

2.1 Direct problem

In the first part, the function v represents a well-posed direct problem without any external force. In mathematical physics, a direct problem involves modeling physical fields like electromagnetic, acoustic, seismic, wave, or heat transfer. It aims to find a function describing the field or process at any location and time, especially if non-stationary. In this study governed by the homogeneous partial differential equation ($v_{tt} = v_{xx}$). Numerically, we employ the Finite Difference Method (FDM) using the initial condition given in equation (2), together with one of the boundary conditions specified in equations (3), (5), (7), or (9), as discussed in [1],[4],[5],[11],[14],[15].

$$v_{i+1,j} = r^2(v_{i+1,j} + v_{i-1,j}) + 2(1 - r^2)v_{i,j} - v_{i,j-1}, \quad i = 1, 2, \dots, (M-1), \\ j = 1, 2, \dots, (N-1) \quad (11)$$

$$v_{i,0} = u_0(x_i), \quad i = 0, 1, \dots, M, \quad v_0(x_i) = \frac{v_{i,1} - v_{i,-1}}{2\Delta t}, \quad i = 1, 2, \dots, (M-1) \quad (12)$$

Six different boundary conditions listed in Table 1 are analyzed. This section describes how each condition is discretized and specifies where they are applied in **Problems 1–6**:



Problems 1 and 3: $v_{0,j} = p_0(t_j), \quad v_{M,j} = p_L(t_j), \quad j = 1, 2, \dots, N \quad (13)$

Problems 2 and 6: $v_{0,j} = p_0(t_j), \quad \frac{\partial v}{\partial x}(L, t_j) = \frac{3v_{M,j} - 4v_{M-1,j} + v_{M-2,j}}{2\Delta x} = q_L(t_j), \quad j = 1, 2, \dots, N \quad (14)$

Problems 4 and 5: $\frac{\partial v}{\partial x}(0, t_j) = \frac{4v_{1,j} - v_{2,j} - 3v_{0,j}}{2\Delta x}, \quad v_{M,j} = p_L(t_j), \quad j = 1, 2, \dots, N \quad (15)$

by using equation (11) with $j = 0$ and using (12) we obtain

$$v_{i,1} = \frac{1}{2} r^2 (u_0(x_{i+1}) + u_0(x_{i-1})) + (1 - r^2) u_0(x_i) + \Delta t v_0(x_i), \quad j = 0, 1, \dots, N, \quad (16)$$

where $v_{i,j} = v(x_i, t_j)$, $x_i = i\Delta x$, $t_j = j\Delta t$ and $r = c\Delta t/\Delta x$, for $i = 0, 1, \dots, M$, $j = 0, 1, \dots, N$, in addition $\Delta x = \frac{L}{M}$ and $\Delta t = \frac{T}{N}$, such that divide the domain $(0, L) \times (0, T)$ into M and N [2]-[4],[6],[7],[11],[15].

2.2 Inverse and III-posed problem:

This section discusses the inverse problem (w, f) using the Finite Difference Method (FDM). Address inverse and ill-posed problems in real situations, like estimating epicardial potentials from surface measurements in electrocardiography or identifying obstacles via inverse scattering of far-field patterns. Inferring causes from effects is an inverse problem. These challenges are often ill-posed, meaning solutions may not exist, may be multiple, or be very sensitive to measurement errors, leading to inaccuracies. Where $w(x_i, t_j) = w_{i,j}$ and $f_i = f(x_i)$. It introduces new work in this research for solving $w_{tt} = w_{xx} + f(x)$ with zero initial and boundary conditions

$$w_{i,j+1} - \Delta t^2 f_i = r^2 (w_{i-1,j} + w_{i+1,j}) + 2(1 - r^2) w_{i,j} - w_{i,j-1} \quad i = 1, \dots, (M-1), \\ j = 1, 2, \dots, (N-1) \quad (17)$$

$w(x_i, 0) = w_{i,0} = 0$, $w_t(x_i, 0) = 0$; **Problems 1 and 3:** $w(0, t_j) = w(L, t_j) = 0$;

Problems 2 and 6: $w(0, t_j) = w_x(L, t_j) = 0$; **Problems 4 and 5:** $w_x(0, t_j) = w(L, t_j) = 0$;

$$w_{i,1} - \frac{1}{2} \Delta t^2 f_i = \frac{1}{2} r^2 (w_{i+1,0} + w_{i-1,0}) + (1 - r^2) w_{i,0} + \Delta t w_t(x_i), \quad j = 0, \\ i = 1, \dots, (M-1). \quad (18)$$



The values of $w_{i,j}$ and f_i must be determined, which means an additional row and column need to be added. To do this, we used an extra condition in equations (4), (6), (7), (9), and (10), plus finding $v_x(0, t_j)$, $v(L, t_j)$, $v_x(0, t_j)$, $v(0, t_j)$, and $v_T(x_i)$ from equations (11-16), we derive the following extra condition to determine $(w(x, t), f(x))$:

Problem 1: $w_x(L, t_j) = q_L(t_j) - v_x(L, t_j), \quad j = 0, 1, \dots, N$ (19)

Problem 2: $w(L, t_j) = p_L(t_j) - v(L, t_j), \quad j = 0, 1, \dots, N$ (20)

Problem 3: $w_x(0, t_j) = q_0(t_j) - v_x(0, t_j), \quad j = 0, 1, \dots, N$ (21)

Problem 4: $w(0, t_j) = p_0(t_j) - v(0, t_j), \quad j = 0, 1, \dots, N$ (22)

Problems 5 and 6: $w(x_i, T) = u_T(x_i) - v_T(x_i), \quad i = 0, 1, \dots, M$ (23)

Given the linearity of the system, the variables $w_{i,j}$, for $i = \overline{1, (M-1)}$ and $j = \overline{1, N}$ can be eliminated, thereby reducing the problem to an ill-conditioned system of N equations with $(M-2)$ unknowns, having a generic structure

$$\underline{Af} = \underline{b},$$

A represents the system matrix, and b denotes the right-hand side vector. Since the system is overdetermined, such that for (30) apply the method of least squares to obtain an approximate solution

$$\underline{f} = (A^T A)^{-1} A^T \underline{b}. \quad (24)$$

Here, the superscript T indicates the transpose operation. Existence and uniqueness were established in [1],[2],[11].

2.2.1 Stability:

As outlined in the theory, all conditions apply, but the key task is to check stability. Most challenges in solving ill-posed problems arise from solution instability. As a result, the term "ill-posed problems" is frequently used to refer to unstable problems. To check stability, we introduce noise as an additional condition, as described in equations (4), (6), (7), (9), and (10) for **Problems 1, 2, 3, and 4**, respectively. The noise is modeled using a Gaussian normal distribution with a mean of zero and a standard deviation σ , as defined for each problem in equations (26)-(30). The noise levels typically



used, according to the literature, are {1%, 3%, 5%}, and we use these values in our analysis. The process is implemented using MATLAB programming, employing the function “normal”:

Problem 1: $w_x^\epsilon(L, t_n) = q_L^\epsilon(t_n) - v_x(L, t_n) = w_x(L, t_n) + \epsilon, \quad n = 1, 2, \dots, N$ (25)

$$q_L^\epsilon(t_n) = q_L(t_n) + \epsilon; \quad \sigma = p\% \times \max_{t \in [0, T]} |q_L(t)|$$

Problem 2: $w^\epsilon(L, t_n) = p_L^\epsilon(t_n) - v(L, t_n) = w(L, t_n) + \epsilon, \quad n = 1, 2, \dots, N$ (26)

$$p_L^\epsilon(t_n) = p_L(t_n) + \epsilon; \quad \sigma = p\% \times \max_{t \in [0, T]} |p_L(t)|$$

Problem 3: $w_x^\epsilon(0, t_n) = q_0^\epsilon(t_n) - v_x(0, t_n) = w_x(0, t_n) + \epsilon, \quad n = 1, 2, \dots, N$ (27)

$$q_0^\epsilon(t_n) = q_0(t_n) + \epsilon; \quad \sigma = p\% \times \max_{t \in [0, T]} |q_0(t)|$$

Problem 4: $w^\epsilon(0, t_n) = p_0^\epsilon(t_n) - v(0, t_n) = w(0, t_n) + \epsilon, \quad n = 1, 2, \dots, N$ (28)

$$p_0^\epsilon(t_n) = p_0(t_n) + \epsilon; \quad \sigma = p\% \times \max_{t \in [0, T]} |p_0(t)|$$

Problems 5 and 6: $w_T^\epsilon(x_m) = u_T^\epsilon(x_m) - v_T(x_m) = w_T(x_m) + \epsilon, \quad m = 1, 2, \dots, M$ (29)

$$u_T^\epsilon(x_m) = u_T(x_m) + \epsilon; \quad \sigma = p\% \times \max_{x \in [0, L]} |u_T(x)|$$

As previously stated, this noise renders the solution unstable, as seen in the numerical result and discussion section. To address this problem, we use zeroth-order Tikhonov regularization (for more information, see [2],[3],[11]).

$$\underline{f}_\lambda = (A^{tr} A + \lambda I)^{-1} A^{tr} \underline{b}^\epsilon, \quad (30)$$

Where λ is a regularization parameter and I is an identity matrix.

3. NUMERICAL RESULT AND DISCUSSION

To evaluate the impact of varying boundary conditions on the accuracy of the finite difference method (FDM) solution, we utilize the same example as presented in [2],[4],[5],[6],[7],[11].

$$u(x, t) = \sin(\pi x) + t + \frac{t^2}{2}, \quad f(x) = 1 + \pi^2 \sin(\pi x), \quad x \in [0, 1] \quad (31)$$

$$u(x, 0) = u_0(x) = \sin(\pi x), \quad u_t(x, 0) = v_0(x) = 1, \quad x \in [0, 1] \quad (32)$$

Problem 1: $u(0, t) = p_0(t) = t + \frac{t^2}{2}, \quad u(1, t) = p_L(t) = t + \frac{t^2}{2}, \quad t \in [0, 1]$ (33)

$$u_x(L, t) = q_L(t) = -\pi, \quad t \in [0, 1]. \quad (34)$$

Figure 1 shows the same results as [4, Fig. 1a]. We've included it here to demonstrate that the program has been used again, but this time with a different approach for the second part, which we refer to as the "inverse part". In addition, Figure 1 presents the numerical results for $v_x(L, t)$ obtained from equations (11)-(16), with input data (32) and (33), computed using the finite difference method (FDM) for three different grid resolutions, namely $M = N = \{20, 40, 80\}$.

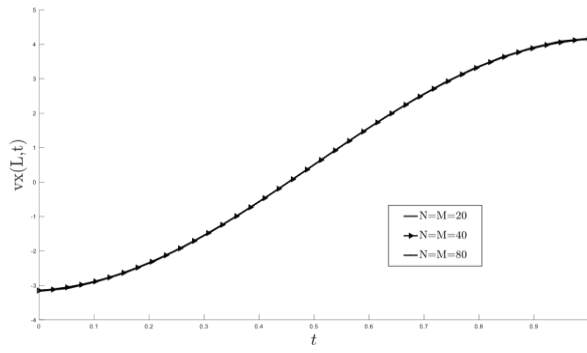


Figure 1. The numerical results for $v_x(L, t)$ under the Dirichlet boundary condition (33) with grid sizes $N = M = \{20, 40, 80\}$.

The numerical result $v_x(L, t)$, as seen in the above figure, is used to obtain the numerical $f(x)$, which means $f(x)$ through (24), obtained by applying zero initial and boundary data, the numerical solution $v_x(L, t)$ from (19), (17), and (18), using grid sizes $M = N = \{20, 40, 80\}$. Figure 2 shows the results, which agree well with the exact answer (31). Comparing [4, Fig. 3a] yields similar results; however, this study uses the finite difference method (FDM), while [4] employed the separation of variables method, suggesting that FDM provides accurate approximations

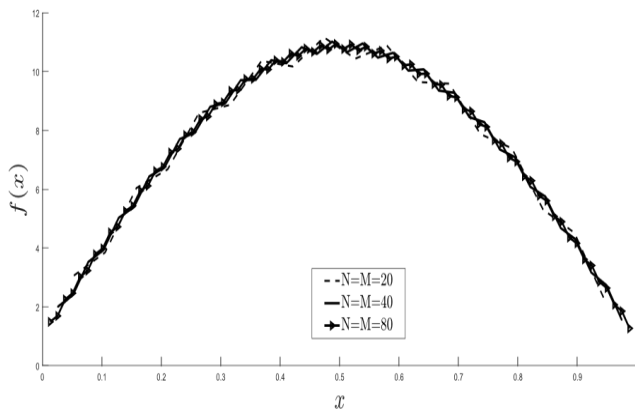


Figure 2. The exact solution (31) for $f(x)$ is compared with the numerical solution obtained from (24), where the Dirichlet boundary condition (33) is applied.

After introducing noise to the data (34) as described in (25), Figure 3 presents the resulting unstable numerical solutions for $f(x)$ at different noise levels $p = \{1, 3, 5\} \%$. The figure clearly demonstrates that increasing noise deteriorates both the stability and accuracy of the reconstruction, highlighting the ill-posed nature of the inverse problem and the necessity of employing regularization techniques to achieve reliable solutions

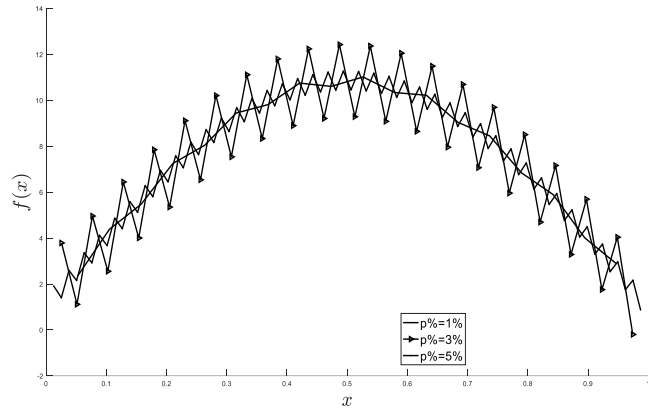


Figure 3. The exact solution (31) for $f(x)$ is compared with the numerical solution (24) for $p = \{1, 3, 5\} \%$, using noisy data.

For a stable result, we use zeroth-order Tikhonov regularization (30). We've tested several values of the regularization parameter λ , including $\{5 \times 10^{-6}, 10^{-6}, 6 \times 10^{-5}, 10^{-5} \dots 10^0\}$. To find the optimal value of λ , we calculate the norm error (35) [1],[4],[14],[16].

$$\| f_{numerical} - f_{exact} \| = \sqrt{\sum_{n=1}^N (f_{numerical}(t_n) - f_{exact}(t_n))^2} \quad (35)$$

Figures 4 and 5 demonstrate that the optimal value for accurately approximating $f(x)$, which is very close to the exact solution, is $\lambda = 1 \times 10^{-8}$. This also highlights that the numerical issue $(w(x, t), f(x))$ can be effectively addressed using the finite difference method (FDM). Additionally, this value of λ differs from the one presented in [4, Fig.5a].

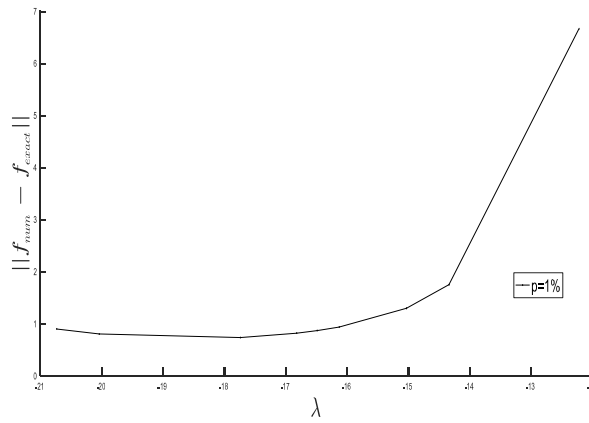


Figure 4. The norm error $\| f_{numerical} - f_{exact} \|$ is presented as a function of λ for $M = N = 80$ and noise $p\% = 1\%$, following the application of the Tikhonov regularization technique. The outcomes are displayed under boundary condition (33).

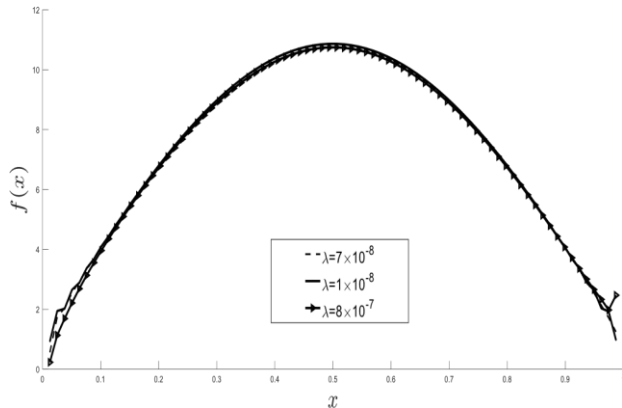


Figure 5. A comparison is carried out between the exact solution of $f(x)$ (31), and the numerical solution obtained for $M = N = 80$ with $p\% = 1\%$ noise for $\lambda \in \{7 \times 10^{-8}, 1 \times 10^{-8}, 8 \times 10^{-7}\}$.

Note: We do not provide approximations for $u(x, t)$ because our numerical results closely match those in [2] and [7].

Problem 2: $u(0, t) = p_0(t) = t + \frac{t^2}{2}, \quad u_x(L, t) = q_L(t) = -\pi, \quad t \in [0, 1] \quad (36)$

$$u(L, t) = p_L(t) = t + \frac{t^2}{2}, \quad t \in [0, t]. \quad (37)$$

First, use the FDM (11)-(16) with input data (32) and (36) for $M = N = \{20, 40, 80\}$ to find the numerical solution $v(L, t)$. Although no exact analytical solution is available for direct comparison, the results indicate convergence and confirm the FDM's effectiveness in capturing the behavior of $v(L, t)$ under the given conditions (36). Then, in [4, Fig. 1b], a similar result can be observed. As shown in our Figure 6, there is a strong resemblance, confirming the consistency between the two approaches.

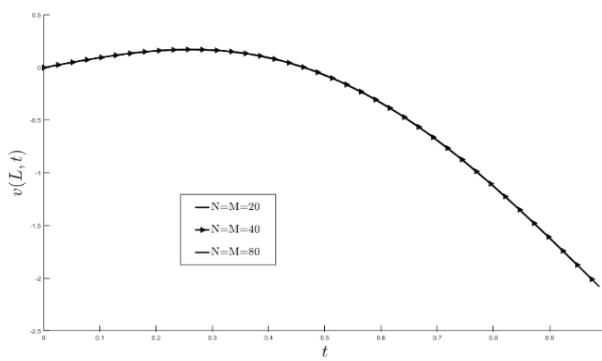


Figure 6. The numerical results for $v(L, t)$ under the mixed boundary condition (36), using the FDM with $M = N = \{20, 40, 80\}$.

Second, using the numerical value of $v(L, t)$ from (20) and the input data in (37), we calculate the numerical solution of $f(x)$ from equation (24). The accuracy and reliability of the FDM are confirmed by the results in Figure 7, which show excellent agreement with the exact solution (31) for $M = N = \{20, 40, 80\}$. The similarity between the two approaches is further emphasized by the comparable trend in [4, Fig. 3b], which closely resembles our Figure 7. Notably, despite our study using the FDM and [4] using the method of variable separation, both methods **producat** the same result.

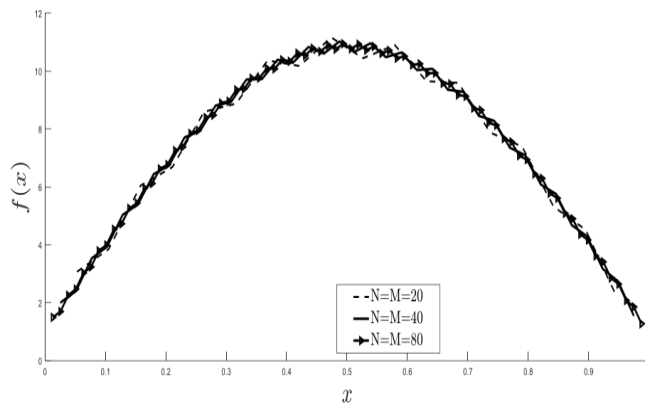


Figure 7. The exact solution (31) for $f(x)$ is compared with the numerical solution obtained from (24), with $M = N = \{20, 40, 80\}$.

Third, we introduce noise to the input data (37), as shown in (26) for stability analysis. The unstable numerical solutions for $f(x)$ at a noise level of $p\% = 1\%$ are presented in Figure 8, illustrating how noise affects the reconstruction's accuracy and stability. A similar result can be seen in [4, Fig. 4b].

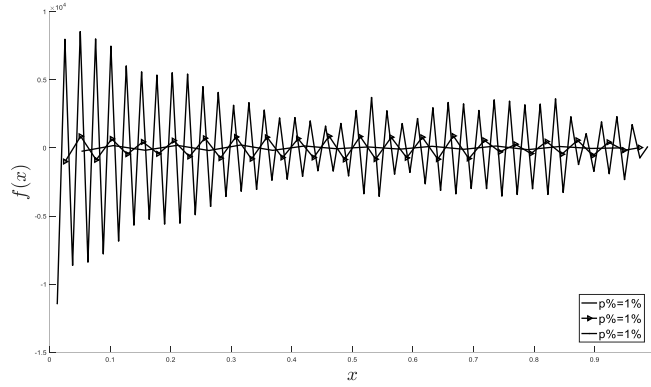


Figure 8. Comparison of the exact solution (31) and the numerical solution (24) $f(x)$, with noisy data at $p\% = 1\%$ and $M = N = 80$.

Finally, to stabilize the solution, we have used zeroth-order Tikhonov regularization, as seen in (30). After testing a range of values for the regularization parameter $\lambda = \{5 \times 10^{-4}, 10^{-4}, 5 \times 10^{-3}, 10^{-3}, \dots, 10^0\}$, the norm error (35) was utilized to identify the optimal value λ . Our findings demonstrate that $\lambda = 3 \times 10^{-5}$ is the ideal choice, as demonstrated in Figures 9 and 10, where the error is minimized. However, [4, Fig. 5b] shows a different value of λ . This likely stems from differences in method, parameter selection, or numerical implementation.

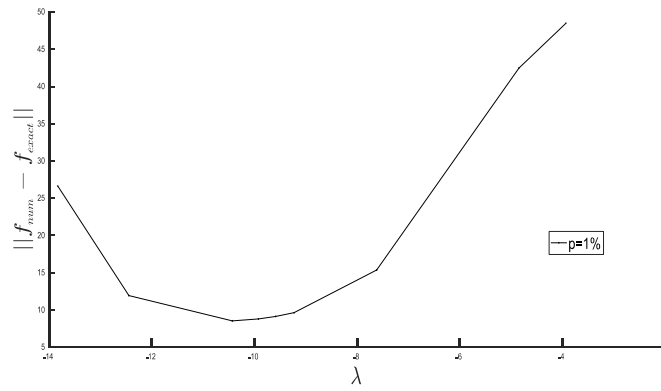


Figure 9. The error $\|f_{numerical} - f_{exact}\|$ is presented as a function of λ for $M = N = 80$ and noise level $p\% = 1\%$.

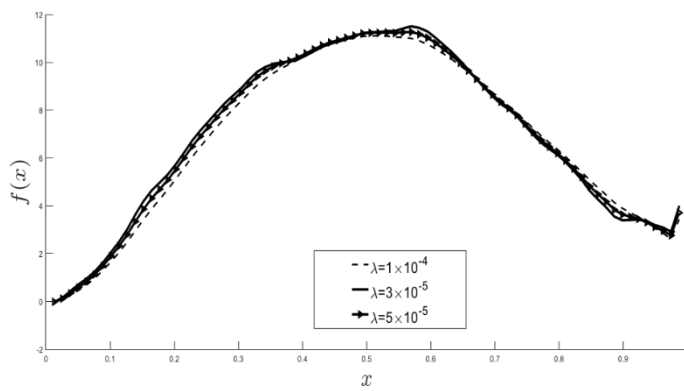


Figure 10. A comparison is made between the exact solution $f(x)$ (31), and the numerical solution (30) obtained for $M = N = 80$ with a noise level of $p\% = 1\%$ for $\lambda \in \{1 \times 10^{-4}, 3 \times 10^{-5}, 5 \times 10^{-5}\}$.

Problem 3: Using the same boundary condition (33) with an extra condition:

$$u_x(0, t) = q_0(t) = \pi, \quad t \in [0, 1] \quad (38)$$

Following the same procedure as in **Problems 1 and 2**, we have determined $v_x(0, t)$, as illustrated in Figure 11, where the numerical results for $v_x(0, t)$ computed under boundary condition (33) and initial condition (32) using the FDM (11)-(16) with $M = N = \{20, 40, 80\}$. A similar outcome, matching [5, Fig. 1a], is observed when comparing it to existing research results.

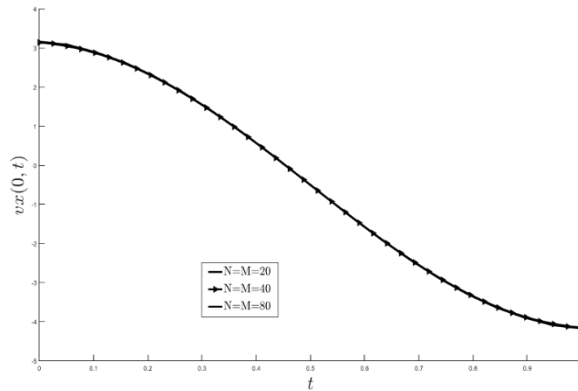


Figure 11. The numerical results for $v_x(0, t)$ using the FDM with $M = N = [20, 40, 80]$, for **Problem 3**.

After that compute the numerical solution of $f(x)$ by (24) under the addition condition (38) as (21) and using FDM (17) and (18) with zero addition and boundary condition at $M = N = \{20, 40, 80\}$. Figure 12 demonstrate excellent agreement between the numerical and exact solutions of $f(x)$ (the noise-free results ($\epsilon = 0$)), thereby confirming the accuracy and reliability of the FDM. It is confirmed

that the shape shown in [5, Fig. 3a] matches our Figure 12. We mainly used the FDM, while [5] combined the separation of variables with their method.

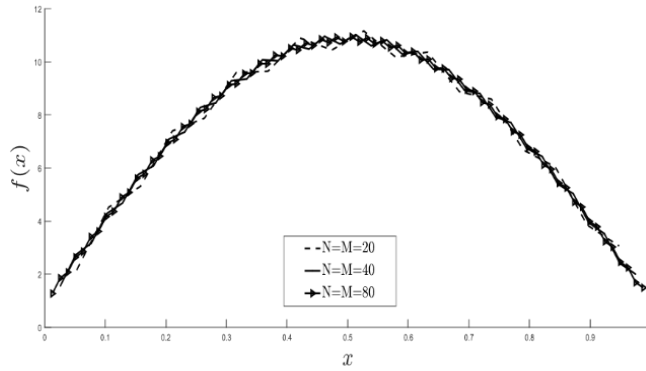


Figure 12. The exact solution (31) of $f(x)$ is compared with the numerical solution (24) for $M = N = \{20, 40, 80\}$, for **Problem 3**.

In order to verify stability, we have introduced noise into the additional condition (38) as shown in (27). A result similar to Figure 8 from **Problem 2** has been noted and is not shown. Using (30) to stabilize the solution, we evaluated several choices of λ and chose the one that minimized the norm error (35), $\lambda = 1 \times 10^{-6}$ is the optimum value, as Figures 13 and 14 illustrate. The difference in λ between [5, Fig. 6a] and this one illustrates the application of the FDM in contrast to the variable separation in [5] for the second part (inverse part).

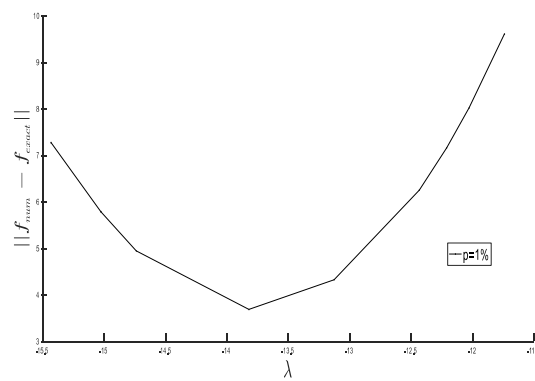


Figure 13. As a function of λ the accuracy error $\|f_{numerical} - f_{exact}\|$ for $M = N = 80$ and noise level $p\% = 1\%$ is obtained after applying the Tikhonov regularization approach, for **Problem 3**.

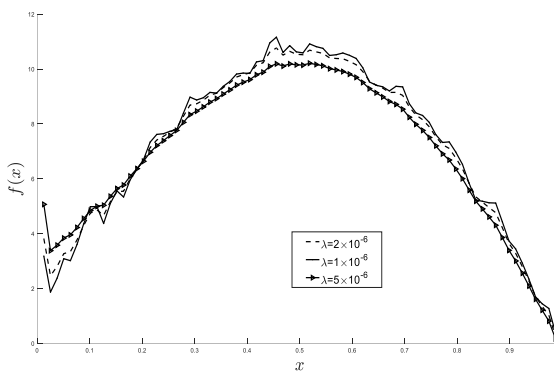


Figure 14. The exact and numerical solution for $f(x)$ at $M = N = 80$ with a noise level of $p\% = 1\%$ for $\lambda \in \{1 \times 10^{-6}, 2 \times 10^{-6}, 5 \times 10^{-6}\}$, for **Problem 3**.

Problem 4: $u(1, t) = p_L(t) = t + \frac{t^2}{2}, \quad u_x(0, t) = q_0(t) = \pi, \quad t \in [0, 1] \quad (39)$

$$u(0, t) = p_0(t) = t + \frac{t^2}{2}, \quad t \in [0, 1] \quad (40)$$

Using the FDM (11)-(16) with $M = N = \{20, 40, 80\}$, the numerical results for $v(0, t)$, presented in Figure 15, were obtained under the initial condition (32) and boundary condition (39). [5, Fig. 1b] shows a similar result.

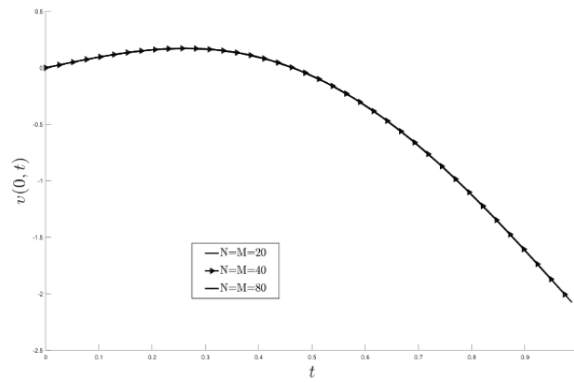


Figure 15. The numerical results for $v(0, t)$ using the FDM with $M = N = \{20, 40, 80\}$, for **Problem 4**.

A similar pattern is observed in [5, Fig. 3b], which closely resembles our Figure 16, confirming the consistency between the two approaches (i.e. FDM and separation variable), where Figure 16 compares the numerical solution of $f(x)$ derived from equation (24) for **Problem 4** with the exact solution provided by equation (31).

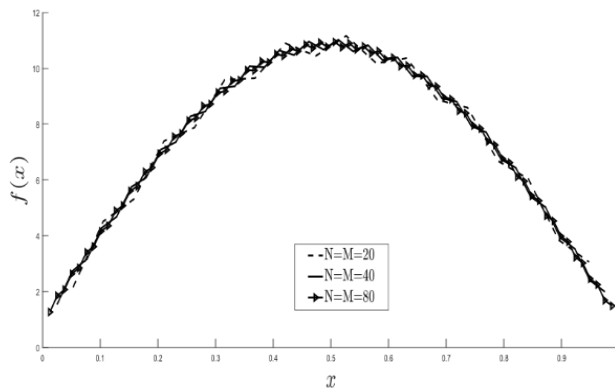


Figure 16. The numerical solution (24) for $M = N = \{20, 40, 80\}$ is compared with the exact solution (31) of $f(x)$, for **Problem 4**.

For the noise term, a result similar to Figure 8, as observed in **Problems 2 and 3**, has been seen and is therefore not included here. Regarding stability, we have followed the same steps as in **Problems 1–3**, but with a different boundary condition (39) and an additional condition (40). The optimal λ has been identified as $\lambda = 2 \times 10^{-4}$, as shown in Figures 17 and 18. Additionally, different λ are illustrated in [5, **Fig. 6b**].

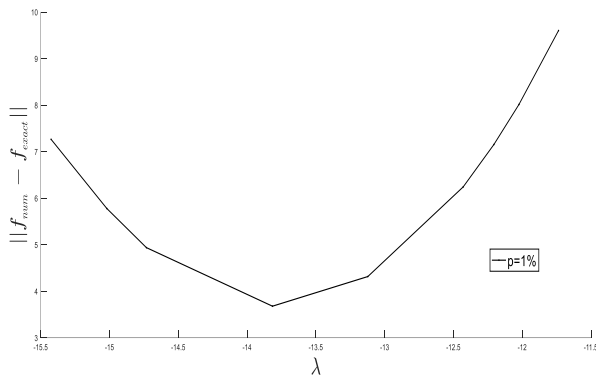


Figure 17. After applying the Tikhonov regularization strategy, the accuracy error $\|f_{numerical} - f_{exact}\|$ for $M = N = 80$ and noise level $p\% = 1\%$ is computed as a function of λ , for **Problem 4**.

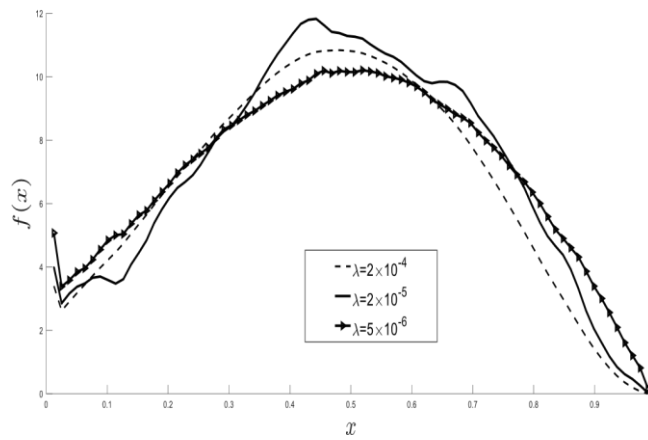


Figure 18. The exact solution $f(x)$ (31) is compared with the numerical solution (30) at $M = N = 80$ with $p\% = 1\%$. The results are presented for $\lambda \in \{5 \times 10^{-6}, 2 \times 10^{-5}, 2 \times 10^{-4}\}$, for **Problem 4**.

Problem 5 and 6: Boundary conditions (39) from Problem 4 and (36) from **Problem 2** have been applied to **Problems 5 and 6**, respectively.

$$u(x, T = 1) = u_T(x) = \frac{3}{2} + \sin(\pi x), \quad x \in [0, 1]. \quad (41)$$

The equations (11)-(16) of the FDM, combined with input data (32) and the boundary conditions (39) for **Problem 5** and (36) for **Problem 6**, have been used to get $v_T(x)$ in Figure 19 a and Figure 19b for $M = N = \{20, 40, 20, 40, 80\}$ (refer to [3],[4],[6] and [7] for additional details). In addition, [6, Fig. 1a] for **Problem 5** and [6, Fig. 1b] for **Problem 6** show a similar result.

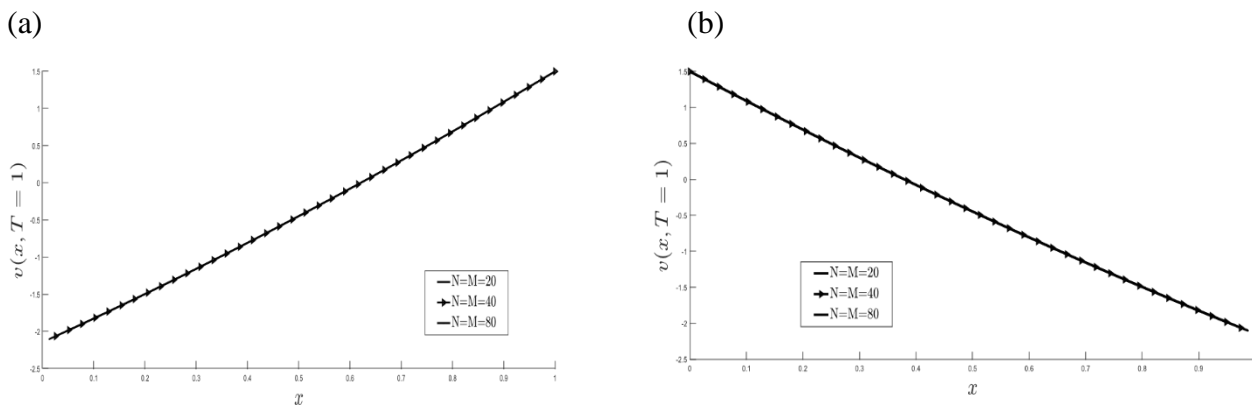


Figure 19. The numerical results for $v_T(x)$ using the FDM with $M = N = \{20, 40, 80\}$, (a) for **Problem 5**, (b) for **Problem 6**.

Next, for $M = N = \{20, 40, 80\}$, we calculate the force $f(x)$. The numerical results from equation (24) using the FDM (17)-(18), with zero initial and boundary conditions and input data (41) as in (23) (such that (39) for **Problem 5**; (36) for **Problem 6**), are compared to the exact solution (31) for both **Problems 5** and **6** in Figure 20, because of their similarities one figure shows $f(x)$ for both **problems 5** and **6**. Our Figure 20 corresponds closely to the results presented in [6, Fig. 6a] for **Problem 5** and [6, Fig. 6b] for **Problem 6**. The separation of variables method is employed in [6], whereas our approach relies on the finite difference method (FDM). To evaluate the stability of the reconstructed force, noise $p\% = 1\%$ has been added to the input data (41), as shown in (29). Since the oscillations observed in the image are similar to those seen in **Problems 2-4**, they have not been included here.

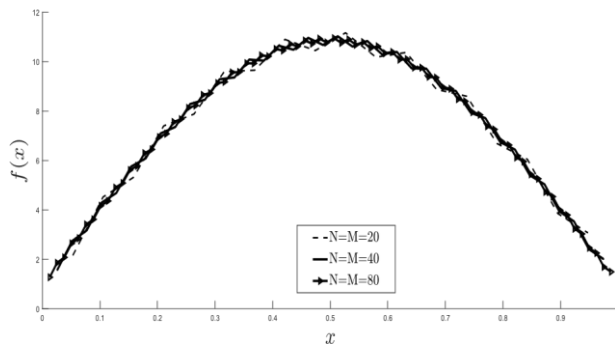


Figure 20: The exact solution (31) for $f(x)$ is compared with the numerical solution (24) with $M = N = \{20, 40, 80\}$, for **Problems 5** and **6**.

Numerous values of λ have been tested to find the optimal value for stability in equation (30). These values include $\lambda \in \{10^{-7}, 5 \times 10^{-7}, 10^{-6}, 3 \times 10^{-6}, 10^{-5}, 4 \times 10^{-5}, \dots, \text{and } 10^0\}$. The minimal norm error (35) has been evaluated for each problem. For **Problem 5**, as shown in Figures 21 and 22, $\lambda = 8 \times 10^{-4}$ has produced the most accurate result; for **Problem 6**, $\lambda = 2 \times 10^{-4}$ has produced the best result, with $f(x)$ closely matching the exact solution, as shown in Figures 21 and 22.

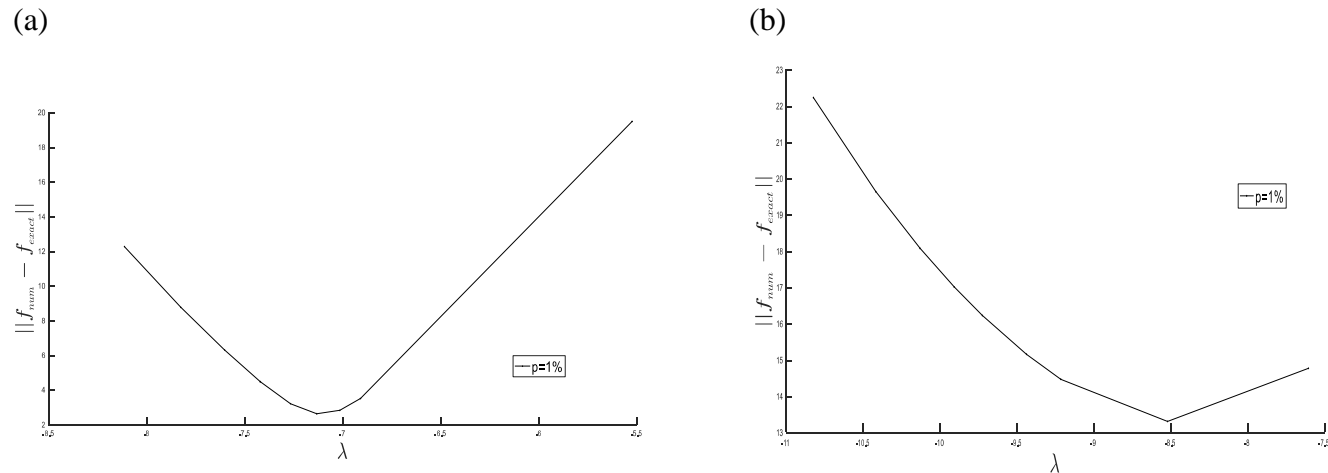


Figure 21: The accuracy error $\|f_{numerical} - f_{exact}\|$ after applying the Tikhonov regularization technique for $M = N = 80$ and $p\% = 1\%$, (a) for **Problem 5**; (b) for **Problem 6**.

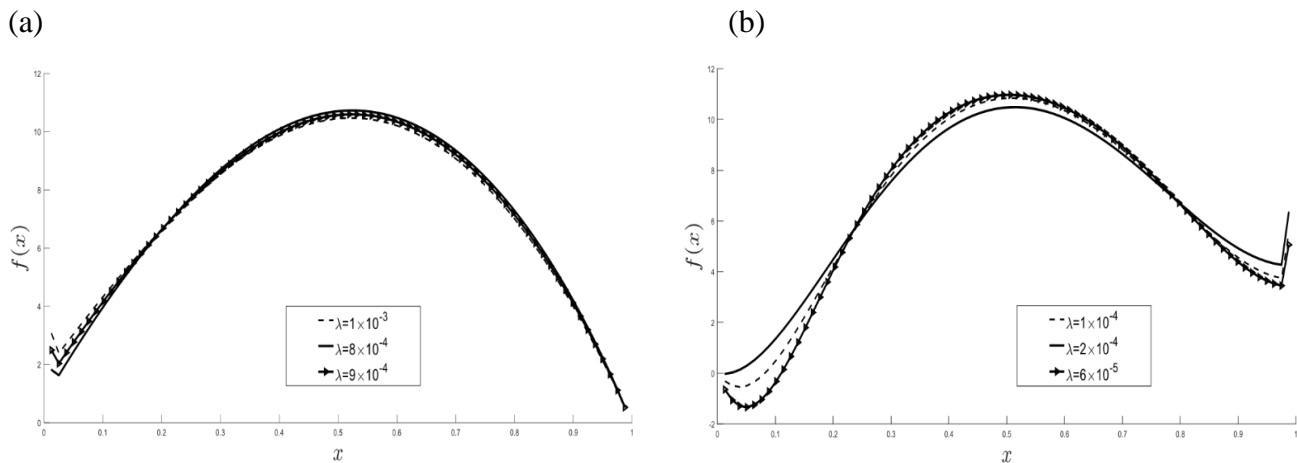


Figure 22: The exact solution (31) for $f(x)$ is compared with the numerical solution (30) for $N=M=80$ and $p\% = 1\%$, and various regularization parameters (a) $\lambda \in \{1 \times 10^{-3}, 8 \times 10^{-4}, 9 \times 10^{-4}\}$, using for **Problem 5**, (b) $\lambda \in \{1 \times 10^{-4}, 2 \times 10^{-4}, 6 \times 10^{-5}\}$ have compared with the exact solution (31) for $f(x)$, for **Problem 6**.

4. CONCLUSION

This study divided the non-homogeneous PDE into two parts: the direct problem and the inverse problem, both of which were solved using the Finite Difference Method (FDM). In addition, this research also showed that the finite difference method effectively solves homogeneous and non-homogeneous partial differential equations under various conditions, providing accurate, stable results. Meanwhile, investigated six problems, each presenting different boundary conditions and additional data. Introducing even a small amount of noise into the supplementary data renders the resulting force unstable, indicating that the problem was ill-posed. To overcome this issue, the Tikhonov regularization method employed, with the regularization parameter selected by minimize the norm error. The non-homogeneous term was originally considered as a single function, $f(x)$, but future research will expand it to include the form $h(x, t)f(x) + g(t)$.

Conflict of interests:

There are non-conflicts of interest.

References

- [1] J. R. Cannon and D. R. Dunninger, "Determination of an unknown forcing function in a hyperbolic equation from over specified data," *Analisi Mathematica Pure Appl.*, vol. 1, pp. 49–62, 1970.
- [2] S. O. Hussein and D. Lesnic, "Determination of a space-dependent source function in the one-dimensional wave equation," *Electron. J. Boundary Elem.*, vol. 12, pp. 1–26, 2014.
- [3] S. O. Hussein and D. Lesnic, "Determination of forcing function in the wave equation. Part I: the space-dependent case," *J. Eng. Math.*, vol. 96, pp. 115–133, 2016.
- [4] S. O. Hussein and M. S. Hussein, "Splitting the one-dimensional wave equation, Part II: Additional data are given by an end displacement measurement," *Iraq J. Sci.*, pp. 233–239, 2021.
- [5] S. O. Hussein, "Splitting the one-dimensional wave equation. Part I: Solving by finite difference method and separation variables," *Baghdad Sci. J.*, 2020, ISSN 2078-8665.
- [6] S. O. Hussein, "Inverse one-dimensional wave equation problem under upper-base as additional information," *Ital. J. Pure Appl. Math.*, pp. 596–608, 2022.
- [7] F. Dou and P. Lu, "An inverse Cauchy problem of a stochastic hyperbolic equation," *arXiv*, (later published in *J. Inverse Probl.*, vol. 41, no. 4, Mar. 17, 2025).
- [8] S. Ngoma, "Well-posedness and Tikhonov regularization of an inverse source problem for a parabolic equation with an integral constraint," *J. Inverse Ill-Posed Probl.*, 2024.
- [9] G. Lin, W. Zang, Z. Ruan, and H. Xu, "Iterative fractional Tikhonov-Landweber method for identifying unknown source on a columnar symmetric domain," *Comput. Appl. Math.*, 2024.
- [10] S. O. Hussein, *Inverse Force Problems for the Wave Equation*, Ph.D. dissertation, Univ. of Leeds, Leeds, U.K., 2016.
- [11] J. L. Lions, *Optimal Control of Systems Governed by Partial Differential Equations*. New York, NY, USA: Springer, 1971.
- [12] M. Yamamoto, "Reconstruction formula and regularization for an inverse source hyperbolic problem by control method," *Inverse Probl.*, vol. 11, no. 3, pp. 481–496, 1995.
- [13] D. Colton and R. Kress, *Inverse Acoustic and Electromagnetic Scattering Theory*, 3rd ed. New York, NY, USA: Springer-Verlag, 2013.
- [14] P. M. Morse and H. Feshbach, *Methods of Theoretical Physics*. New York, NY, USA: McGraw-Hill, 1953.



- [15] C. H. Huang, "An inverse non-linear force vibration problem of estimating the external forces in a damped system with time-dependent system parameters," *J. Sound Vib.*, vol. 242, no. 4, pp. 749–765, 2001.
- [16] M. S. Hussein, *Coefficient Identification Problems in Heat Transfer*, Ph.D. dissertation, Dept. Appl. Math., Univ. of Leeds, Leeds, U.K., 2016.
- [17] Z. Y. Peng, Y. Zeng, and T. D. Chuong, "Solution stability and well-posedness for classes of parametric set optimization problems," *J. Optim. Theory Appl.*, 2025.
- [18] C. H. Huang *et al.*, "An inverse non-linear force vibration problem of estimating the external forces in a damped system with time-dependent system parameters," *J. Sound Vib.*, vol. 242, pp. 749–765, 2025.
- [19] H. Zhan, "Well-posedness problem of an anisotropic parabolic equation with a nonstandard growth order," *Adv. Continuous Discrete Models*, Art. no. 55, Dec. 2024.



خلاصة

مقدمة: في هذه الدراسة، تُحل معادلة تقاضلية جزئية غير متجانسة من الدرجة الثانية إلى جزء متجانس وجزء غير متجانس. تقدم الأبحاث السابقة حول وجود وتقدير الحلول لكلا القسمين أساساً رياضياً واضحاً.

طرق العمل: نستخدم طريقة الفروق المحدودة لحل كلٍ من المكونات المتجانسة وغير المتجانسة عددياً. وقد أخذت في الاعتبار شروط حدودية مختلفة، بما في ذلك شروط ديريشلية ونيومان والشروط المختلطة، وكل منها يتطلب معلومات تكميلية محددة. لتقدير استقرار الحلول العددية، ندخل مستويات موضوعات مختلفة ونطبق تنظيم تيخونوف لثبت النتائج.

الاستنتاجات: تُقدم العديد من الأمثلة العددية لتقدير فعالية النهج المقترن. تشير النتائج إلى أن طريقة الفروق المحدودة تُعطي حلولاً دقيقة في ظل مجموعة من الشروط الحدودية، وأن تنظيم تيخونوف يعزز الاستقرار بشكل فعال في البيئات الصالحة.

الخلاصة: ثبتت النتائج العددية ممانة وموثوقية الطريقة المقترنة. من خلال الجمع بين تنظيم تيخونوف وتقدير الفروق المحدودة، تُرسى هذه الدراسة إطاراً فعالاً لحل المعادلات التقاضلية الجزئية غير المتجانسة من الدرجة الثانية في ظل ظروف حدودية متنوعة.

الكلمات المفتاحية: المسألة العكسية والمبشرة؛ طريقة الفروق المحدودة؛ التنظيم؛ معادلة تقاضلية جزئية من الدرجة الثانية.